Effect of the Reactive Gas on the Solid-State Transformation of Molybdenum Trioxide to Carbides and Nitrides

Senzi Li, Won Bae Kim, and Jae Sung Lee*

Department of Chemical Engineering and School of Environmental Engineering, Pohang University of Science and Technology, Pohang, Korea 790-784

Received January 15, 1998. Revised Manuscript Received April 23, 1998

A temperature-programmed reaction method was employed to investigate the solid-state transformation of molybdenum oxides to carbides or nitrides by reaction with various reacting gases such as H_2 and NH_3 and the mixtures of CH_4 and H_2 (CH_4/H_2 1/4), CO and H_2 (CO/H_2 1/4), and N_2 and H_2 (N_2/H_2 1/3 and 3/1). The solid-state transformation of MoO_3 to nitride by reaction with NH_3 was topotactic. In contrast, MoO_3 took a nontopotactic route by reaction with the other gases or their mixtures, leading to products that were thermodynamically stable under the investigated conditions. For the synthesis to take a topotactic route it required that the carburization or nitridation occurs in the initial stage of reduction to form intermediate phases containing carbon or nitrogen at low temperatures.

Introduction

Molybdenum nitrides and carbides are active and selective catalysts for a variety of reactions such as hydrogenation of CO and olefins,[1−5] NH_3 synthesis,[6] hydrocarbon re-forming[7,8] and hydrogenolysis of hydrocarbons,[9,10] and hydrotreating.[11−15] Application of these materials as practical catalysts requires them to be prepared with high specific surface areas. There are several ways known to prepare molybdenum nitrides and carbides with high surface areas such as temperature-programmed reactions,[16−19] ultrasonic processing to produce nanostructured carbides,[20,21] and supporting on alumina or zeolites of high surface areas.[22,23]

Temperature-programmed reaction (TPR) between MoO_3 and carbon- or nitrogen-containing reaction gases has been found to be a convenient and efficient method to prepare molybdenum nitride and carbide powders of high specific surface area.[16−19] This method controls elegantly the rate of elementary steps involved in the solid transformation and drives the overall reaction in such a manner that materials with desired properties can be produced. The properties of the resulting materials depend greatly on the synthesis conditions such as the nature of reactive gases, the ramping rate of preparation temperature, the space velocity of reactive gases, and the final temperature of TPR as well as the time for which the sample is exposed at the temperature.

Most frequently, a mixture of CH_4/H_2 or CO/H_2 has been employed as reactive gases for the synthesis of carbides, and ammonia has been employed for nitrides. Ammonia is a unique reductant in that it drives the solid transformation into a topotactic route. Thus, molybdenum nitrides of high specific surface areas have been synthesized by TPR between MoO_3 and NH_3. The produced γ-Mo_2N have a cubic metastable crystal structure and bears pseudomorphism with its parent MoO_3, and it can be further carburized to cubic α-MoC_{1-x}, which is also a metastable phase under the preparation conditions.[19] Recently there has been a report that molybdenum nitride powders with high specific surface areas could also be synthesized by temperature-programmed reaction between MoO_3 and a N_2/H_2 mixture.[24]

In this study, we examined the effect of reactive gas on the solid transformation of MoO_3 to molybdenum carbides or nitrides in the temperature-programmed

* Corresponding author. Phone: 82-562-279-2266. Fax: 82−562-279-5799. Email: jlee@postech.ac.kr.

(1) Logan, M.; Gellman, A.; Somorjai, G. A. *J. Catal.* **1985**, *94*, 60.
(2) Leary, K. J.; Michaels, J. N.; Stacy, A. M. *J. Catal.* **1986**, *101*, 301.
(3) Ranhotra, G. S.; Haddix, G. W.; Bell, A. T.; Reimer, J. A. *J. Catal.* **1987**, *108*, 24.
(4) Lee, J. S.; Yeom, M. H.; Lee, D. S. *J. Mol. Catal.* **1990**, *62*, 145.
(5) Lee, J. S.; Yeom, M. H.; Park, K. Y.; Nam, I.; Chung, J. S.; Kim, Y. G.; Moon, S. H. *J. Catal.* **1991**, *128*, 126.
(6) Volpe, L.; Boudart, M. *J. Phys. Chem.* **1986**, *90*, 4874.
(7) Levy, R. B.; Boudart, M. *Science* **1973**, *181*, 547.
(8) Bridgewater, A. J.; Burch, R.; Michell, P. C. H. *J. Chem. Soc., Faraday Trans. 1.* **1980**, *76*, 1811.
(9) Lee, J. S.; Locatelli, S.; Oyama, S. T.; Boudart, M. *J. Catal.* **1990**, *125*, 157.
(10) Iglesia, E.; Ribeiro, F. H.; Boudart, M.; Baumgartner, J. E. *Catalysis Today*, **1992**, *15*, 307.
(11) Lee, J. S.; Boudart, M. *Appl. Catal.* **1985**, *19*, 207.
(12) Abe, H., Bell, A. T. *Catal. Lett.* **1993**, *18*, 1.
(13) Lee, K. S.; Abe, H.; Reimer, J. A.; Bell. A. T. *J. Catal.* **1993**, *139*, 34.
(14) Ramanathan, S.; Oyama, S. T. *J. Phys. Chem.* **1995**, *99*, 16365.
(15) Choi, J. G.; Brenner, J. R.; Thompson, L. T. *J. Catal.* **1995**, *154*, 30.
(16) Volpe, L.; Boudart, M. *J. Solid State Chem.* **1985**, *59*, 332.
(17) Volpe, L.; Boudart, M. *J. Solid State Chem.* **1985**, *59*, 348.
(18) Lee, J. S.; Oyama, S. T.; Boudart, M. *J. Catal.* **1987**, *106*, 125.
(19) Lee, J. S.; Volpe, L.; Ribeiro, F. H.; Boudart, M. *J. Catal.* **1988**, *112*, 44.
(20) Suslick, K. S.; Choe, S. B.; Cichowlas, A. A.; Grinstaft, M. W. *Nature* **1991**, *353*, 414.
(21) Suslick, K. S.; Hyeon, T.; Fang, M. *Chem. Mater.* **1996**, *8*, 2172.
(22) Lee, J. S.; Boudart, M. *Catal. Lett.* **1993**, *20*, 97.
(23) Solymosi, F.; Szoke, A.; Cserenyi, J. *Catal. Lett.* **1996**, *39*, 157.
(24) Wise, R. S.; Markel, E. J. *J. Catal.* **1994**, *145*, 344.

S0897-4756(98)00022-2 CCC: $15.00
Published on Web 06/10/1998

reaction of MoO_3. The employed reactive gases were H_2 and NH_3 and mixtures of CH_4/H_2, CO/H_2, and N_2/H_2. We monitored the gas-phase concentration by gas chromatography and examined the solid phase by XRD and SEM at various stages of TPR preparation. XRD-monitored changes in crystal structure and the morphology observed by SEM told if pseudomorphoism, a signature of topotaxy, was involved in the solid transformation. A combination of these techniques provided a better understanding of the nature of the solid transformation involved in the synthesis. Particular attention was paid to when and how the topotaxy is involved in the solid transformation.

Experimental Section

Temperature-Programmed Reaction (TPR). A temperature-programmed reaction procedure was employed to investigate the solid-state transformation process involved in the conversion of molybdenum oxide to carbides or nitrides. In all the cases, 1 g of MoO_3 powder (Aldrich, 99.95%) was loaded in a U-shaped quartz reaction cell stuffed with quartz wool at the bottom to hold the powders. The employed reactive gases were NH_3 (Matheson, 99.99%), CO (Alphagaz, 99.5%), CH_4 (Union Carbide, 99.95%), as well as H_2 and N_2, with purity higher than 99.99%. These gases were further purified through 5 Å molecular sieves and oxygen traps (Alltech). A stream of gas or gas mixture was passed through the reaction cell at a total flow rate of 70 μmol s^{-1}. The flow rates were controlled by the mass flow controllers (Brooks). For mixing gases, the mole ratio of CH_4 or CO to H_2 was 1/4 for both, and those for N_2 to H_2 were 1/3 and 3/1, respectively. The preparation temperature was varied in a furnace coupled with a PID controller and was monitored locally with a thermocouple. Following rapid heating to 573 K in 0.5 h, samples were further heated to the indicated temperatures with a linear ramping rate of 60 K h^{-1}.

Identification and analysis of gaseous reaction products were carried out by an online HP 5890A gas chromatograph (GC) equipped with a thermal conductivity detector (TCD) and a mass spectrometer (HP 5972 MSD). Porapak Q (Alltech) packed in a stainless steel tube (1 m × 3.2 mm OD) was used as the column material for product analysis of carbide syntheses and Porapak N (Alltech) for nitride syntheses. Oven temperatures were maintained isothermally at 423 K during the whole analysis procedure. Sample injection to GC was performed every 5 min using a six-port sampling valve attached on the streamline.

Methods of Characterization. Since fresh molybdenum carbide and nitride powders burned spontaneously upon exposure to air, samples were passivated prior to characterization by letting the air diffuse slowly into the reaction cell with one end of the reactor open to atmosphere for 10 h to get a mild surface oxidation.

The specific surface areas (S_g) of the samples were determined by the N_2 BET method on a Micromeritics ASAP 2010C adsorption analyzer. The passivated samples were degassed at 473 K under vacuum for 8 h prior to surface area measurements.

To examine the structural evolution process during the TPR preparation, powder X-ray diffraction (XRD) measurements were conducted using a Mac Science M18XHF diffractometer with Cu Kα radiation (λ = 1.5418 Å). The variation of the gas-phase concentrations was monitored by gas chromatography. When major changes of gas concentrations occurred, the TPR process was stopped and the sample was quenched. XRD measurements were then conducted to examine the solid structure at that point. The procedure was repeated to observe the structural evolution on several intermediate points during the preparation. The morphology of the passivated samples was observed by scanning electron microscopy (SEM) on a JEOL JSM-840A.

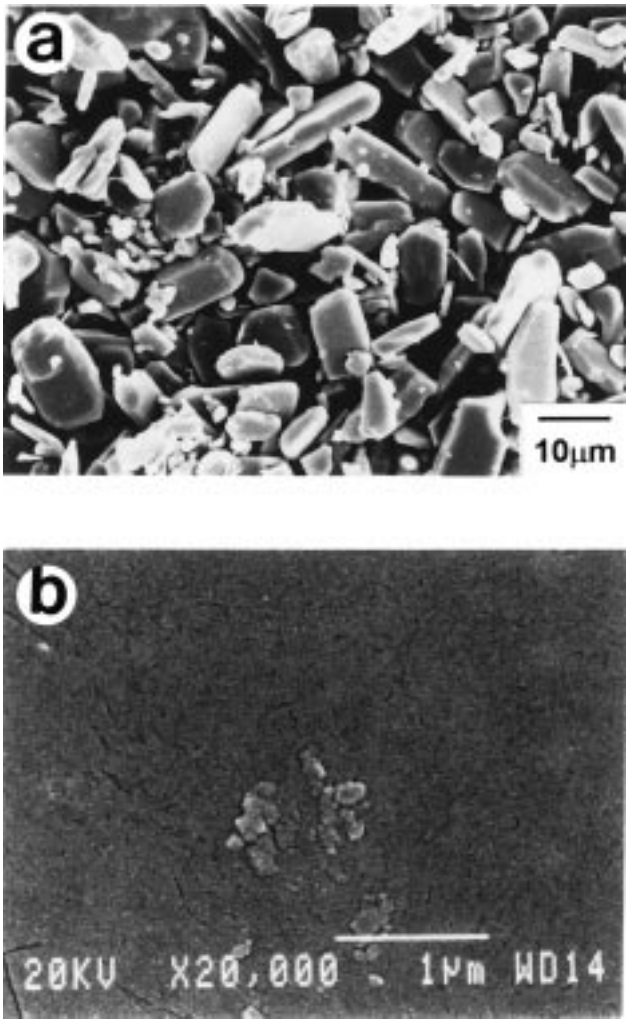

Figure 1. Scanning electron micrographs showing morphology of precursor MoO_3 (Aldrich, 99.95%): (a) overall morphology and (b) focused on the face of a platelet.

Results

Precursor MoO_3. Molybdenum trioxide has an orthorhombic crystal structure with surface area of ca. 1 m^2 g^{-1}. It consists of layers of MoO_6 octahedra sharing corners and edges.[25] Since the layers are held together by van der Waals forces, grinding in a mortar with a pestle or smearing on the stub when preparing samples for XRD or SEM measurements could crush it. Typically, MoO_3 is of platelet shape, although the size along different dimensions may vary depending upon preparation methods that manufacturers employ. The morphology of MoO_3 employed in this study (Aldrich) is illustrated in the SEM micrograph shown in Figure 1a. Most of platelets show a length greater than 10 μm. Focusing on the surface of one platelet and increasing the magnification to 20 000 times shows a large number of cracks and defects (Figure 1b), indicative of the roughness of the MoO_3 surface, which would facilitate the reaction between gas-phase molecules and the solid.

Reactions with H_2 and CH_4/H_2 (1/4). Figure 2 shows the TPR trace of water formation during the solid transformation of MoO_3 by reaction with H_2. Two H_2O peaks, indicating the reduction of MoO_3, are observed

(25) Toth, L. E. *Transition Metal Carbides and Nitrides*; Academic Press: New York, 1971.

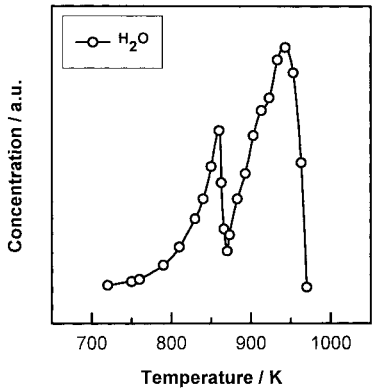

Figure 2. Temperature-programmed reaction (TPR) profile of the transformation of MoO_3 with H_2 (ramping rate = 60 K h^{-1}, H_2 flow rate = 70 μmol s^{-1}, MoO_3 loading = 1 g).

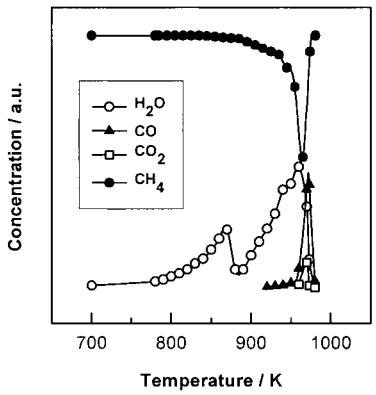

Figure 3. Temperature-programmed reaction (TPR) profile of the transformation of MoO_3 with CH_4/H_2 (1/4) (ramping rate = 60 K h^{-1}, total gas flow rate = 70 μmol s^{-1}, MoO_3 loading = 1 g).

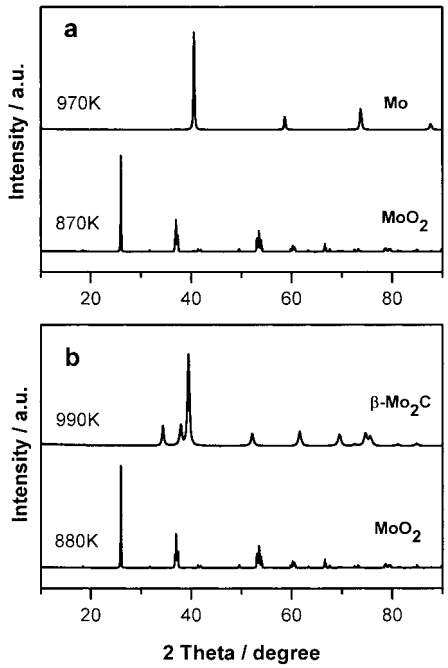

Figure 4. XRD patterns showing the structural evolution of MoO_3 by TPR with (a) H_2 and (b) $CH_4/4H_2$.

when the reaction proceeds from 700 to 970 K. In agreement with previous report,[18] XRD patterns (Figure 4a) confirm the formation of a pure phase of MoO_2 at 870 K and metallic Mo at 970 K, respectively. The trace of H_2O formation as a function of temperature and the XRD identification demonstrate that the reaction proceeds in two steps: MoO_3 is first reduced to MoO_2 and then directly reduced to the final product, metallic Mo.

Figure 3 gives the formation traces of H_2O, CO, and CO_2, and the consumption trace of CH_4 during the TPR of MoO_3 with a gas mixture of CH_4 and H_2 (1/4) A similar trace of H_2O formation to that shown in Figure 2 is obtained, implying their similar reduction pathway. No CH_4 is consumed below 880 K, illustrating that CH_4 is not involved in the reaction below this temperature. The XRD pattern (Figure 4b) shows that MoO_2 is the only phase at 880 K. Thus, the solid transformation of MoO_3 below 880 K, the first stage of reduction, is proved to be the reduction of MoO_3 to MoO_2 by H_2. In contrast to the role of CH_4 acting as a spectator at the first stage of reduction, CH_4 begins to be consumed above 880 K, and a great amount of CO and trace amount of CO_2 are released with concomitant consumption of CH_4 at temperatures above 950 K. The XRD peaks, characteristic of the hexagonal-close-packed (hcp) phase of β-Mo_2C (Figure 4b), identify the formation of the carbide at the end of the TPR (970 K). This behavior reveals that CH_4 serves as both reduction and carburization agents at temperatures between 880 and 990 K, the second stage of reduction. Carbon and hydrogen, the two elements constituting a methane molecule, contribute to the reduction of MoO_2, with carbon producing CO and CO_2 and hydrogen yielding H_2O. Meanwhile, carbon is incorporated into the molybdenum lattice to form the molybdenum carbide. There is no indication that metallic Mo is formed as an intermediate of carburization.

As illustrated in Figure 5, SEM photographs show that the morphology changes during the two stages of TPR reactions with H_2 (Figure 5a,b) and with $CH_4/4H_2$ (Figure 5c,d). At 870 and 880 K, when MoO_2 was produced during the TPR of MoO_3 with H_2 and CH_4/H_2 (1/4), respectively, the particles have a totally different morphology from that of MoO_3. So do the morphologies of the products at the end of TPR in both cases.

Reactions with CO/H_2 (1/4). The results of TPR between MoO_3 and a gas mixture of CO and H_2 (1/4) are given in Figure 6. Unlike the TPR with CH_4/H_2 (1/4) a variety of gaseous products are obtained along with a more complicated TPR profile. Although two H_2O peaks are formed, the first stage of reduction occurs at much lower temperatures than that of MoO_3 with H_2 or CH_4/H_2 (1/4). In addition, CO is consumed throughout the synthesis reactions with the highest peak centered at 960 K. CO_2 formation follows roughly the opposite trace of CO consumption, suggesting that CO takes part in the reduction of MoO_3 during the whole transformation process, and its contribution increases markedly at temperatures above 890 K, when the carburization happens. This different behavior of CO from that of CH_4 seems reasonable, because CO is a stronger reductant compared with CH_4, which is quite stable, especially at low temperatures.

Methane and trace C_2 (ethane and ethylene) are present between 700 and 900 K. The formation of CH_4 and C_2 indicates that CO hydrogenation occurs during the transformation process. Interestingly, alternating changes in the concentrations of CO_2 and CH_4 imply a competition between CO hydrogenation and the reduc-

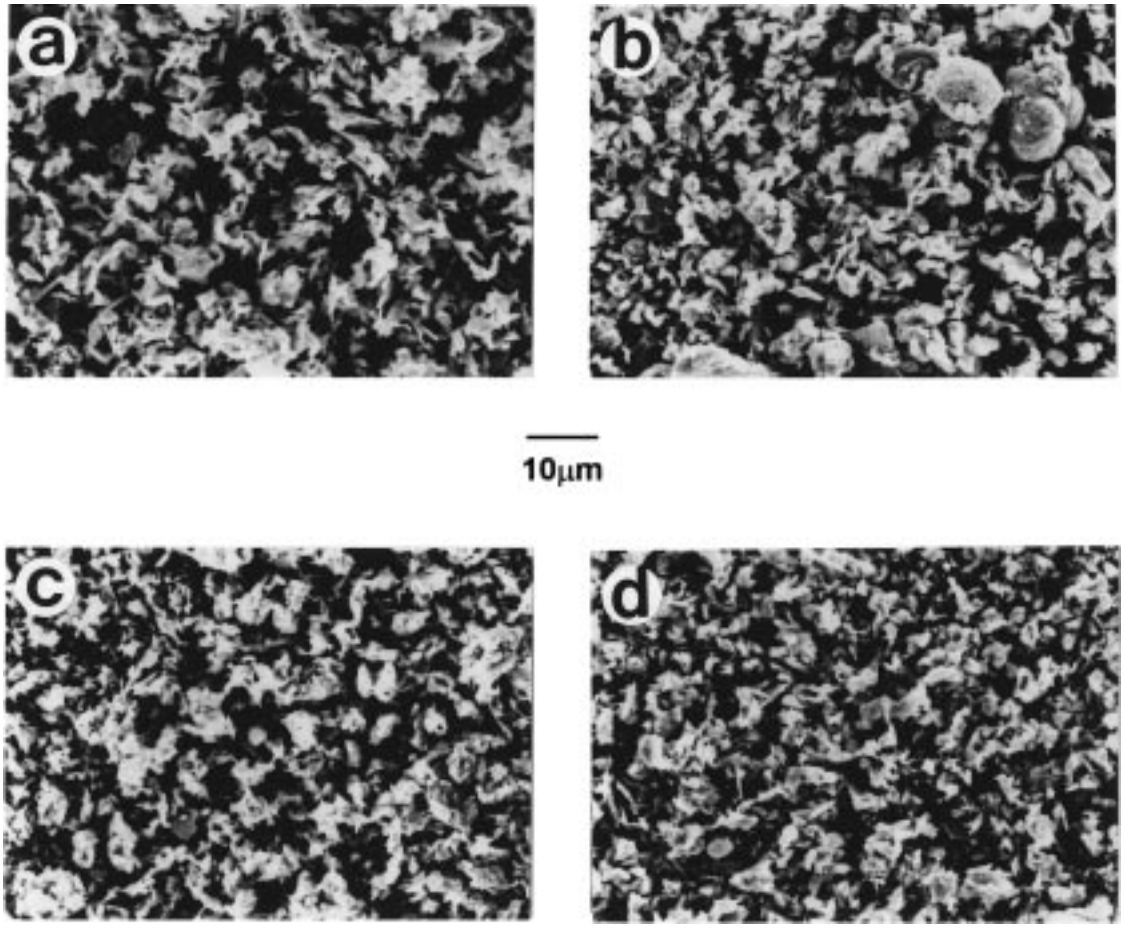

Figure 5. Scanning electron micrographs showing morphology of the transformation of MoO_3 with H_2 at (a) 870 K and (b) 970 K and with CH_4/H_2 (1/4) at (c) 880 K and (d) 990 K.

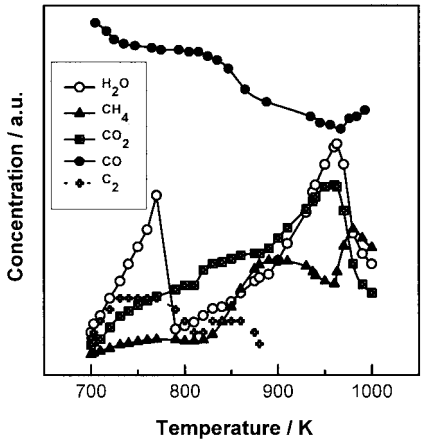

Figure 6. Temperature-programmed reaction (TPR) profile of the transformation of MoO_3 with CO/H_2 (1/4) (ramping rate = 60 K h^{-1}, total gas flow rate = 70 μmol s^{-1}, MoO_3 loading = 1 g).

tion of MoO_3. The CO hydrogenation is significantly suppressed at around 950 K when CO is heavily involved in the reduction and carburization. However, as the reduction and the carburization are almost finished at temperatures above 950 K, a dominating CH_4 formation occurs, suggesting that Mo_2C product is acting as a catalyst for CO hydrogenation.[1,3,5]

As shown in Figure 7, XRD patterns confirm the formation of MoO_2 phase at 890 K and β-Mo_2C (hcp) at 1000 K. Again, no metallic Mo phase is observed. Molybdenum carbide is produced at the end of the TPR

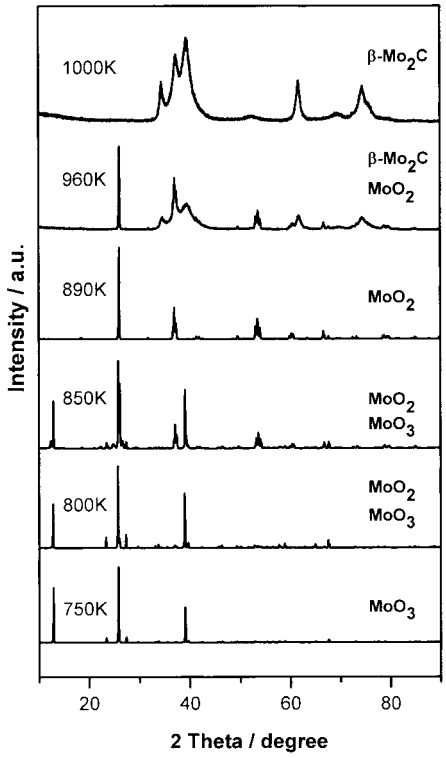

Figure 7. XRD patterns showing the structural evolution of MoO_3 by TPR with CO/H_2 (1/4).

but with much broader diffraction peaks compared with Mo_2C prepared by reaction with CH_4/H_2 (1/4). It should

be mentioned that, despite the varied gaseous products yielded during the TPR of MoO_3 by reactions with CO/H_2 (1/4), its solid transformation goes through two stages similar to those with H_2 and CH_4/H_2 (1/4); i.e., MoO_3 is first reduced to MoO_2 and then further reduced and carburized to β-Mo_2C. In fact, the carburization of MoO_2 by CO occurs only above 890 K, although CO starts to reduce MoO_3 at much lower reaction temperatures than that for CH_4. The slight shifts to higher temperatures of the points at which MoO_3 is completely reduced to MoO_2 and then to β-Mo_2C reflect the lower H_2 partial pressure due to the additional consumption by CO hydrogenation.

It is noticeable that the reduction of MoO_3 by CO/H_2 (1/4) has started below at 750 K (Figure 6). However, there is no XRD evidence for the bulk phases of MoO_2 at this temperature (Figure 7), revealing the amorphous nature of the initial reduction products. Moreover, the morphology of MoO_3 is rarely altered until 750 K (Figure 8a), implying that the reduction of MoO_3 is mostly limited to the surface of the particles at this temperature. Here, the gradual destruction of MoO_3 platelets to particles of irregular shapes can be observed by two other SEM photographs, showing the morphology of MoO_2 formed at 890 K (Figure 8b) and β-Mo_2C produced at 1000 K (Figure 8c) during the TPR with CO/H_2 (1/4). Having no resemblance to the morphology of MoO_3, the product granules appear similar to those formed by reaction with H_2 and with CH_4/H_2 (1/4) (Figure 5). Among the morphologies of MoO_2 and β-Mo_2C presented in the above three TPR processes, magnified views of two typical shapes, the striplike and their agglomerates, are displayed in Figure 9.

Reactions with NH_3. Figure 10 gives the TPR profile of the transformation of MoO_3 to Mo_2N by reaction with NH_3. The trace of H_2O formation shows that the first peak initiates at 650 K and ends at 900 K, while the reaction mostly occurs within a narrow temperature range from 650 to 750 K, which is much lower than those required for the reduction or carburization by other gases. It has been reported that MoO_2 can only react with NH_3 to form Mo_2N at temperatures above 900 K.[25,26] Accordingly, the small amount of H_2O formed above 900 K can be ascribed to the part produced when converting MoO_2 to Mo_2N. Yet, the intensity of this high-temperature peak is much smaller than that of the low-temperature peak. In addition to the formation of H_2O, NH_3 decomposes to yield N_2 above 750 K, and the TPR trace for N_2 formation follows a symmetric trend to that of NH_3 disappearance. Nearly all the ammonia has been consumed or decomposed at 900 K.

XRD patterns showing the structural evolution during MoO_3 nitridation are vastly different from those of the reduction or carburization by other gases (Figure 11). The formation of γ-Mo_2N with face-centered-cubic (fcc) structure is confirmed at the end of transformation. The NH_3 TPR profile shows that the reaction initiates at 650 K, whereas XRD indicates no bulk phases other than MoO_3 present at this temperature. Nevertheless, the phase of MoO_3 vanishes completely by simply increasing the temperature by 50 K. A small amount of MoO_2 phase and an unresolved crystalline phase (called henceforth "phase X") appear at 700 K. The phase of γ-Mo_2N emerges at 750 K, proving that the nitridation with NH_3 occurs at much lower temperatures than the carburization with CH_4/H_2 or CO/H_2. Meanwhile, phase X turns to another unidentified phase (called henceforth "phase Y"). As the temperature further increases, the phases other than γ-Mo_2N gradually diminish, and γ-Mo_2N is the only crystal phase at the end of the TPR.

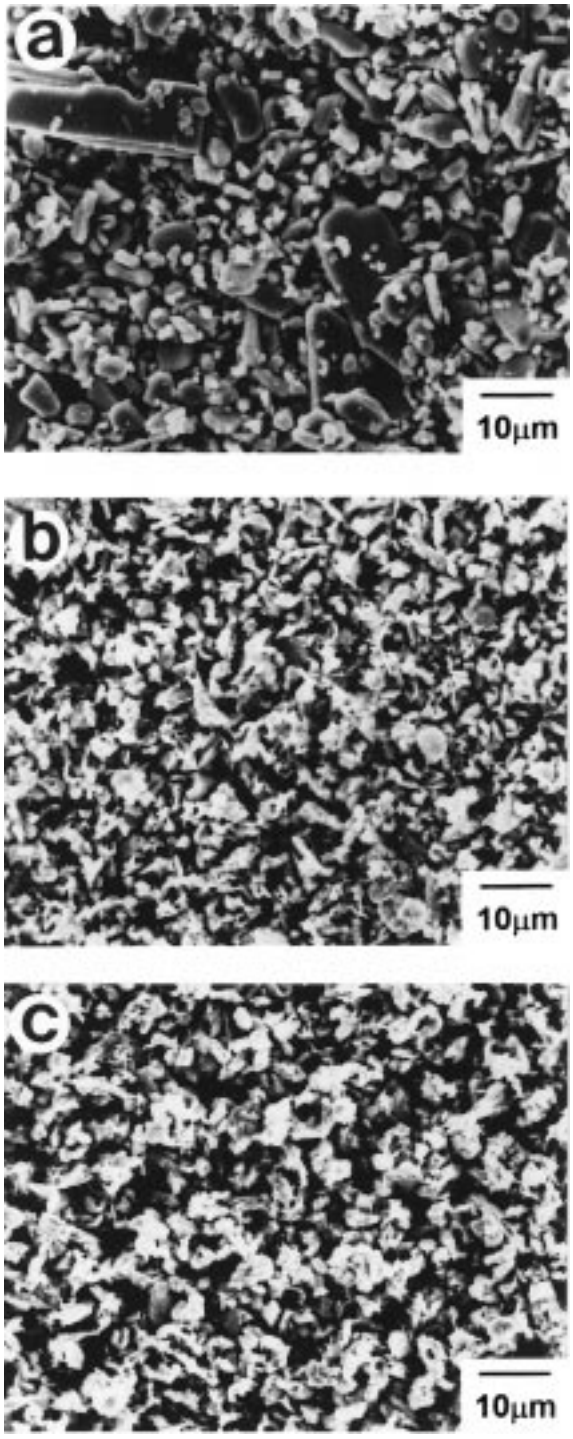

Figure 8. Scanning electron micrographs showing morphology of the transformation of MoO_3 with CO/H_2 (1/4) at (a) 750 K, (b) 890 K, and (c) 1000 K.

The morphology during TPR with NH_3 was observed by SEM. As illustrated in Figure 12, the morphologies during the whole transformation remain unaltered and thus all morphological features of precursor MoO_3 are

(26) Jaggers, C. H.; Michaels, J. N.; Stacy, A. M. *Chem. Mater.* **1990**, *2*, 150.

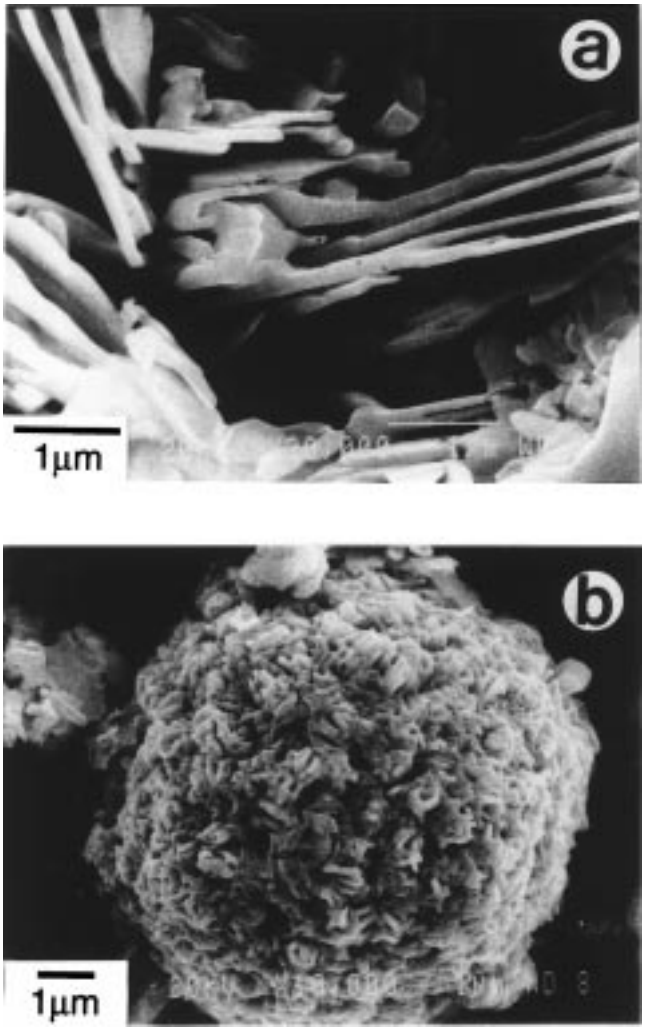

Figure 9. Scanning electron micrographs showing two kinds of typical morphology of MoO_2 and β-Mo_2C: (a) strip-like shape and (b) agglomerated particles.

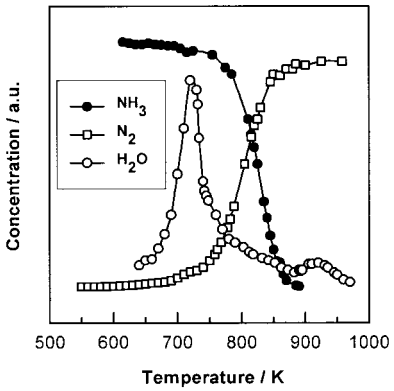

Figure 10. Temperature-programmed reaction (TPR) profile of the transformation of MoO_3 with NH_3 (ramping rate = 60 K h^{-1}, NH_3 flow rate = 70 μmol s^{-1}, MoO_3 loading = 1 g).

preserved in the intermediates and products. Here, three magnified SEM photographs reveal some interesting images of the solids in the early stage of nitridation (Figure 13). Although the overall shape of the sample at 700 K retains that of precursor MoO_3, when the phase of MoO_3 is totally transformed to the phase X, a kind of ripplelike disfigurement occurs on the surface of the platelets. More interestingly, those surface corrugations disappear completely above 800 K, when MoO_2 and

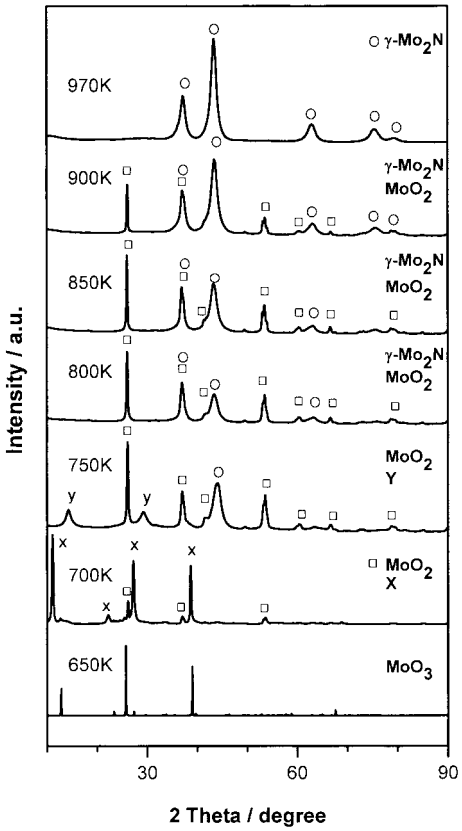

Figure 11. XRD patterns showing the structural evolution of MoO_3 by TPR with NH_3.

γ-Mo_2N are formed as the only phases. The corrugated surfaces reflect the substantial structural evolution during the initial nitridation of MoO_3, while the healing probably can be ascribed to the formation of relatively stable phases. Taking into account the fact that intensive reactions, leading to complete structure changes and a variety of intermediates, take place within a narrow temperature range, it is remarkable that the gross morphology is maintained with only slight transient surface disfigurement.

Reactions with N_2 and H_2. The transformation processes of MoO_3 to nitrides by reactions with a gas mixture of N_2 and H_2 with different mole ratios were also investigated and their TPR profiles are given in Figure 14. In both cases, the two stages of H_2O evolution are similar, except some temperature shifts compared to those of the MoO_3 reduction by reactions with H_2, CH_4/H_2 (1/4) or CO/H_2 (1/4). β-Mo_2N with a tetragonal structure, as identified by XRD, is the final product of both TPR processes (Figure 15). Once more, XRD patterns confirm that MoO_3 is first reduced to MoO_2 and then further reduced and nitrided. Here is another characteristic worth noting: unlike the preparation with CH_4/H_2 (1/4), CO/H_2 (1/4), or NH_3, metallic Mo appears in both TPR processes. Also, the relatively richer H_2 content in the mixture as in the case of N_2/H_2 (1/3) shifts the TPR profile to lower temperatures, leading to more metallic Mo product.

The SEM photographs in Figure 16 show the morphology changes during the two stages of TPR with N_2/H_2 (1/3) (Figure 16a,b) and with N_2/H_2 (3/1) (Figure 16c,d). At 890 and 910 K, when the phases of MoO_2 are formed, the particles show totally different morphol-

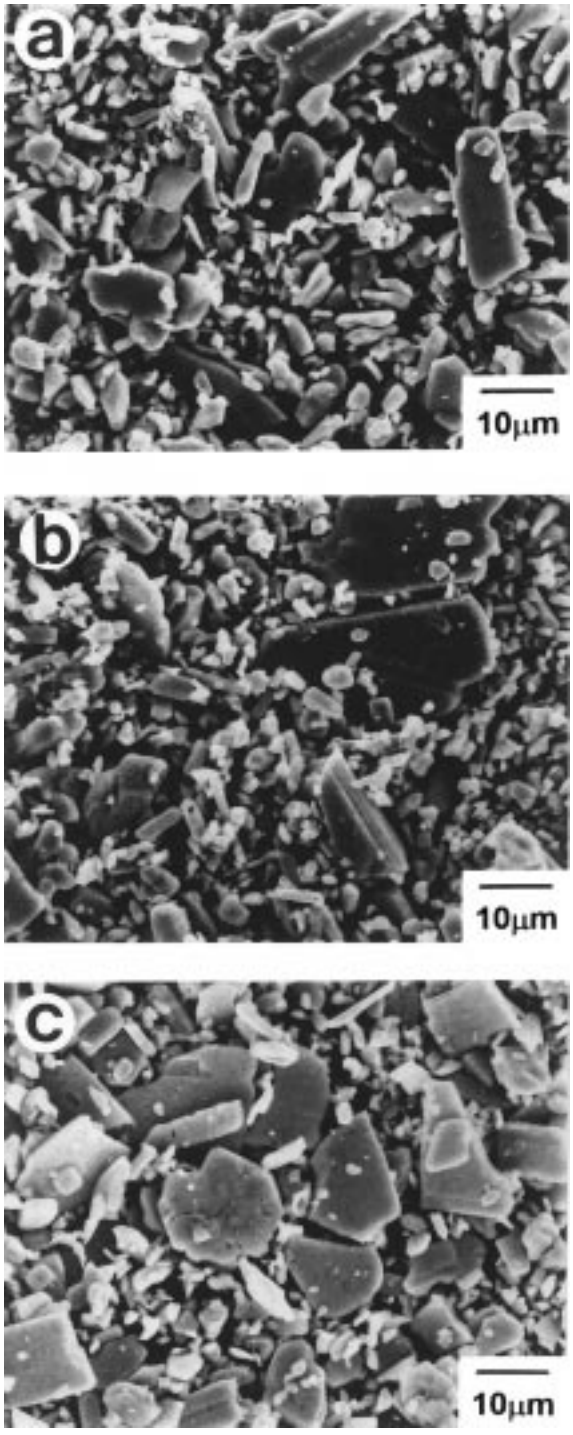

Figure 12. Scanning electron micrographs showing pseudomorphism in the topotactic transformation of MoO_3 to γ-Mo_2N by TPR with NH_3 at (a) 700 K, (b) 850 K, and (c) 970 K.

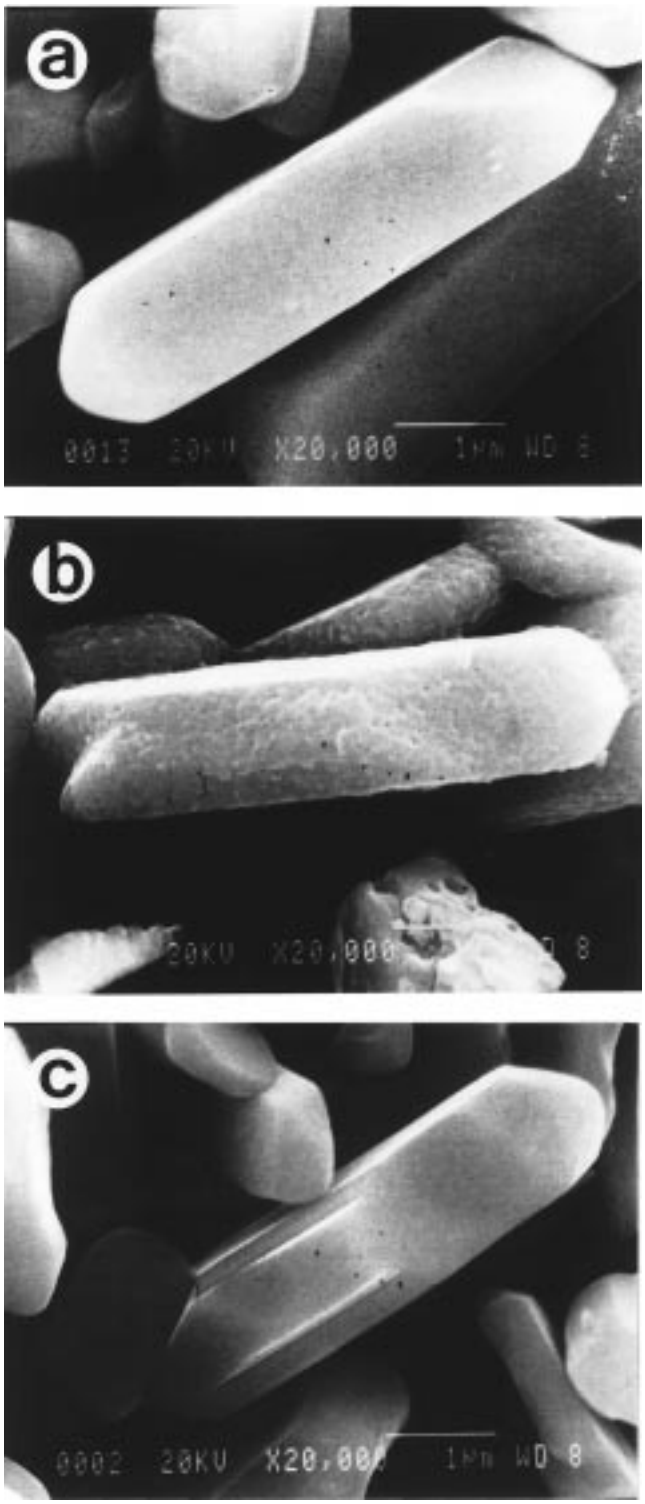

Figure 13. Scanning electron micrographs showing morphology of the transformation of MoO_3 with NH_3 at (a) 650 K, (b) 700 K, and (c) 800 K.

ogy from that of MoO_3. So do the morphologies of the products at the end of TPR in both cases. These morphology changes involved in the reduction of MoO_3 with N_2/H_2 (1/3 and 3/1) are completely different from those in NH_3 TPR, where the product is pseudomorphous to the precursor MoO_3.

Characteristics of the Final Products of TPR. The characterization result of the final products obtained in the TPR transformation of MoO_3 are summarized in Table 1. γ-Mo_2N (fcc) is produced at the end of the TPR of MoO_3 by reaction with NH_3. In contrast, thermodynamically preferred products, β-Mo_2C and β-Mo_2N, are obtained by reaction with other reactive gases. The primary interest of this work was to investigate the structural evolution during the solid transformation. Thus, the preparation conditions were not optimized to obtain high specific surface areas. As a result, the surface areas of the products listed in Table 1 are lower than those usually obtained by the TPR method due to the higher ramping rate and the lower space velocity that we employed for the TPR investigation. Yet, in agreement with previous results,[3,18,19]

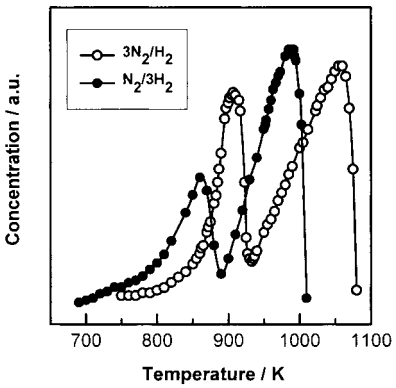

Figure 14. Temperature-programmed reaction (TPR) profile of the transformation of MoO_3 with N_2/H_2 (1/3) and N_2/H_2 (3/1) (ramping rate = 60 K h^{-1}, total flow rate = 70 μmol s^{-1}, MoO_3 loading = 1 g).

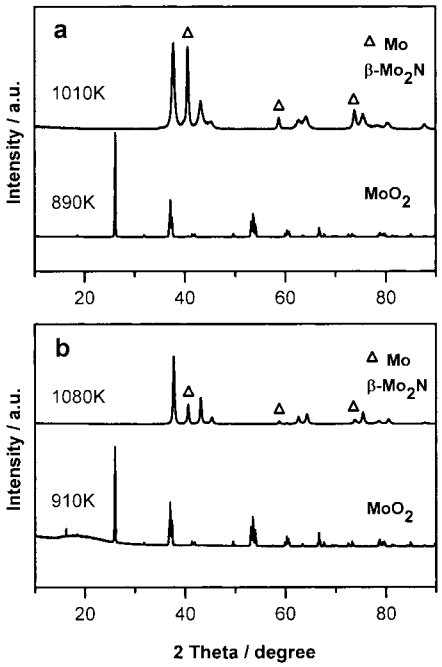

Figure 15. XRD patterns showing the structural evolution of MoO_3 by TPR with (a) N_2/H_2 (1/3) and (b) N_2/H_2 (3/1).

γ-Mo_2N (fcc) possesses a higher surface area than the products obtained with other reacting gases.

Discussion

It has been demonstrated that molybdenum carbide and nitride can be synthesized through a topotactic reaction route from MoO_3.[16−19] The topotaxy is achieved when the solid product has a well-defined crystallographic orientation relative to its parent MoO_3. Thus, the (100) planes of Mo_2N are parallel to the (010) planes of MoO_3, as demonstrated by transmission electron microscopy (TEM) with selected area diffraction (SAD).[17] On scanning electron micrographs, the topotaxy manifests itself with pseudomorphism between the solid product and parent MoO_3.[3,27]

The solid-state transformation involved in a temperature programmed-reaction between MoO_3 and NH_3 to form γ-Mo_2N is topotactic, as indicated by the pseudomorphism between the precursor and the product and by the formation of a thermodynamically metastable phase γ-Mo_2N. Our observations are consistent with the reaction scheme proposed by Volpe and Boudart[16,27] as well as Jaggers et al.[26] for solid transformation from MoO_3 to γ-Mo_2N with NH_3 as a reducing/nitriding agent. Molybdenum trioxide, on its way to γ-Mo_2N, is to be transformed to two intermediate phases, oxynitrides and MoO_2. Taking the first route, NH_3 is adsorbed on the surface and subsequently nitrogen is incorporated into the lattice of molybdenum. Hydrogen is combined with oxygen to form water while nitrogen stays in the lattice interstices. During this process, only nonmetal atoms seem to move in and out of the lattice with molybdenum atoms remaining almost motionless. Most of the MoO_3 is transformed to γ-Mo_2N through a series of metastable oxynitride intermediates, MoO_xN_y. Following the separate parallel route, a fairly small portion of MoO_3 is converted to MoO_2 and then nitrided to Mo_2N. The first route leads to topotactic products with pseudomorphism, while the second route results in nontopotactic products with morphology completely different from that of the precursor. In this study, the topotactic transformation has been illustrated by monitoring morphology changes by SEM (Figure 12). Although some MoO_3 is converted to MoO_2 during the TPR preparation, the amount is so small that its influence on the morphology is negligible. The small contribution of MoO_2 in the reduction of MoO_3 by NH_3 has been reflected in the smaller high temperature peak of TPR shown in Figure 10. In contrast, the high temperature peaks in TPR with other gases in Figures 2, 3, and 6 show roughly twice as much as the intensity of the low-temperature peaks, as expected from the stoichiometry of the reduction process, indicating that MoO_2 is the sole intermediate. XRD peaks of MoO_2 obtained during the TPR of MoO_3 with NH_3 are much narrower than those of phase X or phase Y, suggesting that there exist two parallel routes of different nature. The solid transformation of MoO_3 by reaction with NH_3 is summarized as follows:

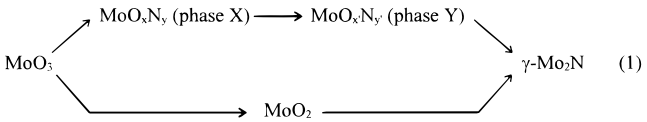

(1)

There is a competition between topotactic and nontopotactic routes. The key point leading to the topotactic route is that the nitridation must occur simultaneously with reduction at low temperatures, i.e., at the initial stage where MoO_3 starts to be reduced. This is a refined criterion for the topotactic synthesis from the previous one which only stipulates that the initial reduction of MoO_3 should take place at low temperatures.[19] Once the phase of MoO_2 were formed, a nontopotactic route would be unavoidable. Accordingly, the nontopotactic products are understood in that MoO_2 has ever appeared as the only phase in the transformation process such as the case of MoO_3 reduction with CH_4/H_2 (1/4) or CO/H_2 (1/4). With CH_4/H_2 (1/4), reduction of MoO_3 to MoO_2 is accomplished by H_2, while CH_4 participates in further reduction and carburization at high temperatures. In the case with CO/H_2 (1/4), CO is involved in the reduction at the beginning of the

(27) Volpe, L.; Boudart, M. *Catal. Rev. Sci. Eng.* **1985**, *27*, 515.

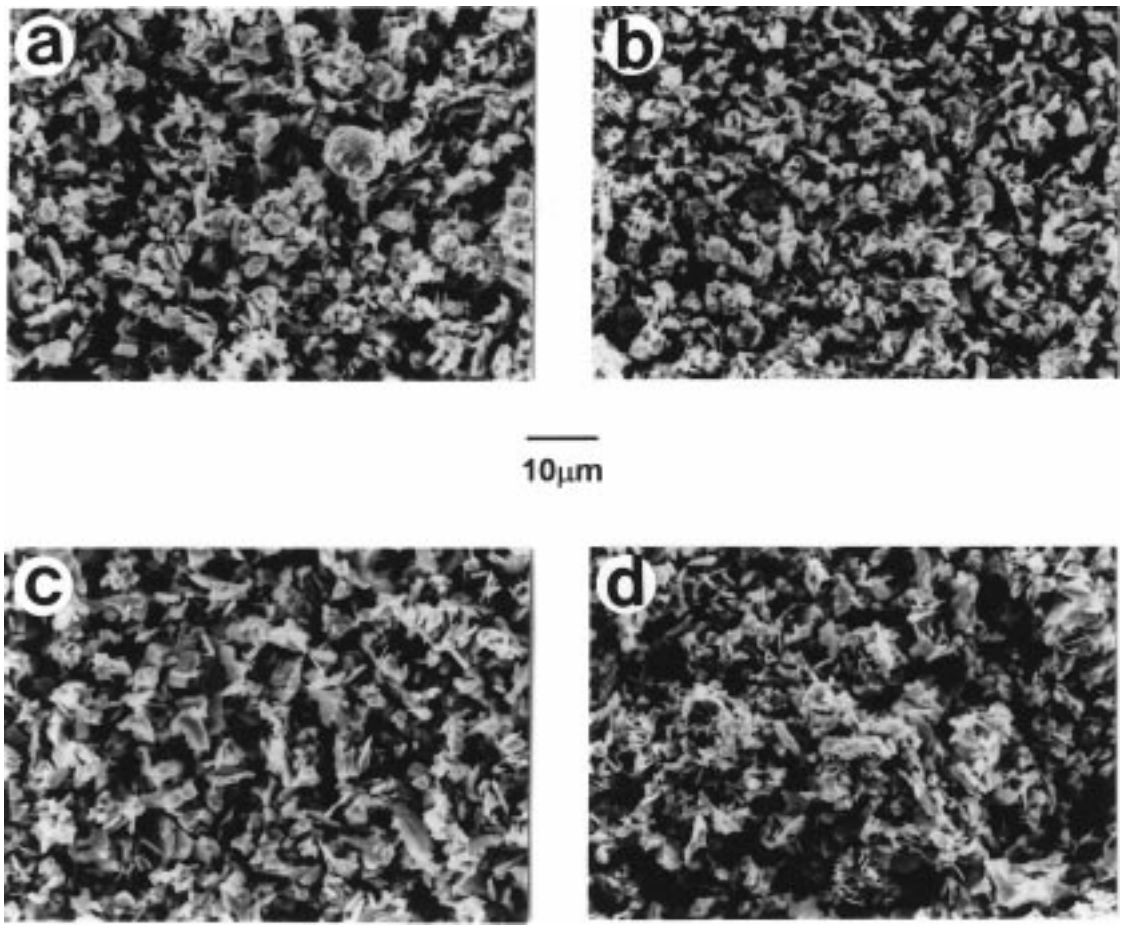

Figure 16. Scanning electron micrographs showing morphology of the transformation of MoO_3 with N_2/H_2 (1/3) at (a) 890 K and (b) 1010 K, and N_2/H_2 (3/1) at (c) 910 K and (d) 1080 K.

Table 1. Characteristics of the Final Products Formed in the TPR of MoO_3 with Various Gases

reacting gas	final temp (K)	surface area ($m^2\ g^{-1}$)	final product	structure
H_2	970	3.5	Mo	cubic
CH_4/H_2 (1/4)	990	3.7	β-Mo_2C	hcp
CO/H_2 (1/4)	1000	7.0	β-Mo_2C	hcp
NH_3	970	10.3	γ-Mo_2N	fcc
H_2/N_2 (3/1)	1010	7.2	β-Mo_2N+Mo	tetragonal
H_2/N_2 (1/3)	1080	6.3	β-Mo_2N+Mo	tetragonal

reaction and initiates the reduction at a lower temperature than with H_2. However, in this first step CO acts as a reductant of MoO_3 to MoO_2 without contributing to carburization. Thus, a nontopotactic route is followed as with CH_4/H_2 (1/4). In both cases, the nature of the solid transformation is determined in the initial stage of MoO_3 reduction, as demonstrated by the morphology change in this stage. The poor crystallinity of Mo_2C produced in TPR with CO/H_2 (1/4) compared to that with CH_4/H_2 (1/4) may probably be ascribed to the simultaneous involvement of several reactions in the transformation process. The solid transformation of MoO_3 by reaction with CH_4/H_2 (1/4) and CO/H_2 (1/4) is summarized as follows:

$$MoO_3 \xrightarrow[CO/H_2]{H_2} MoO_2 \xrightarrow[CO/H_2]{CH_4/H_2} \beta\text{-}Mo_2C \qquad (2)$$

The thermodynamic phase diagram of the Mo−C system[18,25] indicated that hexagonal β-Mo_2C is the only thermodynamically stable carbide under present preparation conditions (C/Mo atomic ratios and temperatures). However, α-MoC_{1-x} with a fcc structure pseudomorphous to MoO_3 has been synthesized by prior impregnation of Pt on MoO_3 and subsequent carburization with CH_4/H_2 (1/4).[19] The same phase could also be obtained by carburization of high surface area γ-Mo_2N. As in the case of topotactic γ-Mo_2N synthesis, the direct α-MoC_{1-x} synthesis also involves the incorporation of carbon into solid matrix in the early stage of MoO_3 reduction. These results reveal that not only the thermodynamically metastable molybdenum nitride but also the metastable carbide phase can be produced under proper conditions.

The basis of topotaxy in a solid transformation is the conservation of a structural motive usually maintained by the relative position of metal atoms. When MoO_3 starts to be reduced, the structural motive is disturbed by departure of some oxygen. If the reduction continues without incorporation of other elements, the stable MoO_2 phase is formed, and all structural motives of MoO_3 are lost during the transformation. When light atoms such as N or C are incorporated into the solid phase and fill the sites vacated by the leaving oxygen, the structural motive of MoO_3 is stabilized, and thus topotactic solid transformation is achieved by progressive incorporation of N or C into the molybdenum lattice as soon as oxygen leaves. This condition requires the presence of atomic nitrogen or carbon at the point of initial MoO_3 reduction. Apparently, ammonia decomposes over MoO_3 itself, and Pt deposited on MoO_3

decomposes CH_4 in the early stage of MoO_3 reduction in the topotactic syntheses of γ-Mo_2N and α-MoC_{1-x}, respectively. Without the help of a metal catalyst, CH_4 and CO stay intact in the first stage of the reduction and play a role of spectator for CH_4 and a reductant and oxygen scavenger for CO, and hence a nontopotactic route is followed.

Molybdenum nitride synthesis with N_2/H_2 is found to take a nontopotactic route, as evidenced by the formation of the MoO_2 intermediate and the absence of pseudomorphism. Unlike other processes, a large amount of metallic Mo intermediate is involved in the solid transformation. Furthermore, the final phase of the solid product is tetragonal β-Mo_2N, whereas both topotactic and nontopotactic synthesis routes with NH_3 produce cubic γ-Mo_2N. It is assumed that nitrogen is incorporated into the solid only after MoO_2 is reduced to metallic Mo. Provided that MoO_2 had been directly converted to the nitride without forming a metallic intermediate, γ-Mo_2N phase would have been obtained, as in the case of nontopotactic NH_3 reduction. The chemical stability of N_2 seems responsible for its delayed participation in the nitridation, allowing the formation of metallic Mo. The solid transformation process of MoO_3 by reaction with N_2/H_2 is summarized as follows:

$$MoO_3 \xrightarrow{H_2} MoO_2 \xrightarrow{H_2} Mo \xrightarrow{N_2} \beta\text{-}Mo_2N \qquad (3)$$

Summary

The solid-state transformation of MoO_3 to γ-Mo_2N by TPR with NH_3 was proved to be topotactic in the sense that the morphology during the TPR was unaltered. In contrast, MoO_3 took a nontopotactic route by reaction with the mixtures of CH_4/H_2 (1/4), CO/H_2 (1/4), and N_2/H_2, leading to β-Mo_2C and β-Mo_2N, which were thermodynamically stable under the investigated conditions. The requirement for the synthesis to follow a topotactic route appeared to be the carburization or nitridation occurring in the initial stage of reduction at low temperatures forming an intermediate containing carbon or nitrogen.

CM9800229